

Process Planning System for an MEMS Device using a 3D Geometric Model

Tomonao Kitahara¹, Satoshi Kanai^{1,2}, Takayuki Shibata² and Takahiro Kawashima²

¹ Division of Systems Science and Informatics, Graduate school of Information Science and Technology, Hokkaido University, Kita 14, Nishi 9, Kita-ku, 060 Sapporo, JAPAN.

Corresponding Author / E-mail: t_kitahara@sdm.ssi.ist.hokudai.ac.jp , TEL: + 81-11-706-6449 , FAX: + 81-11-706-7120

² Graduate School of the Department of Production Systems Engineering, Toyohashi University of Technology, Aichi, JAPAN

KEYWORDS : MEMS, Process Planning, 3D-CAD, ReDesign, Process Feature.

This paper proposes a new 3D process planning system for MEMS device manufacturing. The process planning system can derive fabrication processes from a 3D device model. The system has two characteristic functions. First, that all feasible fabrication process sequences can be derived, and secondly, that some portions of the device model can be automatically modified so that it is easier to fabricate them. Process planning is based on process features that are just one clue to finding precedence in the process sequence of the device.

Manuscript received: July 15, 2009 / Accepted: August 15, 2009

1. Introduction

Recently, because the market for MEMS (Micro Electro-Mechanical Systems) has been developing rapidly, the separation of MEMS device design from its fabrication is expected, and the occasions for MEMS device design seem to be increasing. So, the computer-aided design system is needed for the designers who do not have thorough knowledge of MEMS fabrication processes because it is difficult for them to determine whether a given device structure can be fabricated well or not.

A lot of computer-aided systems for MEMS design have been developed, for example, fault analysis[1], etching simulation[2], and integrated design systems, such as: CoventorWare[3] and MemsONE[4]. The integrated design systems provide etching simulation, integrated electromagnetic-mechanical analysis, process emulation, etc., based on the MEMS device model. However, almost all of these systems do not include a process planning function where feasible fabrication processes for the device can be derived.

On the other hand, only a few prototypes of process planning system prototypes[4-7] for MEMS have been studied as shown in Table 1. However, all of them still have technical limitations. For example, in the systems[4,6], the geometry of the MEMS device structure was only expressed by 2D cross sections. In the systems[5,6,7], material for the device is limited to a single material, and the process is further restricted to surface micromachining. Furthermore, the systems realized[4,6] are a redesigning function of device geometries so that it is easier to fabricate them. Unfortunately, the other systems did not have such functionality. Therefore, a process planning system having higher planning function than those in the previous systems is strongly required.

Overcoming these limitations, the following four requirements should be satisfied in a process planning system for the MEMS device.

Requirement 1) 3D process planning ability

2D cross-sectional representation of the device could not accurately express the 3D MEMS device structure. For this reason, the system

Table 1 Our algorithm and related works

	Req.1	Req.2	Req.3	Req.4	Characteristics of the method
[Jianhua Li et al] [5]	○	×	×	○	Feature of Surface geometry
[Saneet A et al.] [6]	×	×	×	○	Based on Graph grammars
[Sungwook Cho et al] [7]	○	×	×	×	Based on Block segmentation
MemsONE software[4]	×	○	○	×	Similarity search in database
The proposed system	○	○	×	○	Exhaustive search of Process Graph

should express a MEMS device structure using a 3D geometric model and should infer the progressive change of 3D geometries of the device in its fabrication processes.

Requirement 2) Identification of layer materials

The MEMS fabrication process proceeds layer by layer. However, in the MEMS fabrication process, only one material can be deposited in a single deposition process. So, the system should identify the difference of material in each layer, and should estimate in what sequence multiple materials are progressively deposited.

Requirement 3) Treating different kinds of fabrication processes

A MEMS device is fabricated from the combination of different kinds of processes, such as: isotropic and anisotropic etching or dry and wet etching, or the “Liga process” and “wafer junction”. For this reason, a process planning system should derive process plans composed of multiple MEMS processes.

Requirement 4) Design for MEMS fabrication ability

A great geometric restriction due to fabrication is imposed on a MEMS device geometry. For this reason, some portions of the device model can be automatically modified so that it is easier to fabricate.

It is better to develop a process planning system that satisfies all of the above four requirements. However, satisfying the third requirement is very difficult, because the process planning algorithm considering all kinds of existing MEMS fabrication processes that

have become very complex. On the other hand, MemsONE inverse design simulator[4] partly realized the third requirement. In the simulator, process plans of the already existing MEMS device can be retrieved from the process database. The process retrieval is based on a geometric similarity evaluation between a given device and those in the database. However, this system has two problems. First, the sufficient number of the existing fabrication processes has not been stored in the database. Secondly, it is highly probable that no device model exists in a database the geometry of which is similar to the given device.

Therefore, the purpose of our study is to develop a new process planning system for MEMS devices which satisfies the first, second and forth requirements. The developed system can treat a MEMS device model with complex 3D geometry and made of multiple materials. The system has two major characteristic functions. First, all possible fabrication process sequences can be derived. Second, some portions of the device model can be automatically modified so that it is easier to fabricate them. Because the shape of the device is geometrically restricted in the MEMS fabrication processes, the developed functions are indispensable for process planning for the MEMS device.

In section 2, the details of the process planning method are described. Next, in section 3, a case study on the micro-oxide-sensor device is shown, and the effectiveness of the system is verified.

2. Proposed process planning method for MEMS

2.1 Assumption of the Process Planning

In our study, we limited the scope of MEMS fabrication processes to “surface micromachining”. It is a typical fabrication process for many kinds of MEMS devices, which is based on layer by layer depositions. Fig.1 shows the fabrication process sequence of the MEMS hinge device model using surface micromachining. The characteristic of the process is that the device structure has sacrificial layers during fabrication. The sacrificial layers are made of a specific material which is different from that of structural layers, and the sacrificial layers have little effect on other structural layers when they are removed by isotropic etching. Using the sacrificial layers enables the device to have hollow or moving parts. In the paper, we define “one process” as a chain from the structural or sacrificial layer deposition to the resist film removal shown in Fig.1. We refer to “a process plan” as a process sequence which is an ordered list of “processes”. Initial MEMS device model SM is given as a 3D-CAD model with an assembly structure. We define the “z-direction” as the normal direction of a substrate surface, and the “negative-z-direction” as the opposite z-direction.

2.2 Basic idea of Process Planning

Since a MEMS device is fabricated by repeating one process to stack materials layer by layer towards the z-direction, the system has to determine a correct deposition orders of materials used in the device. So, our system performs process planning based on the *process feature* which is a clue to finding the preceding relationship of deposition order. This idea is proposed in the former paper[4]. We modified the idea in this case to develop a new process planning algorithm. A process feature is a specific set of connected faces and edges, which express the characteristic underside of each structural layer.

Fig.2 shows the flow of the process planning which consists of the following four steps:

- (A-1) Process features in a given initial device model are extracted.
- (A-2) A set of *fabrication features* and a *projection overlay relationship matrix* are generated based on the process features.
- (A-3) A set of *process sequences* is generated.
- (A-4) A modified device model and mask geometries fabricated by the one process sequence are derived.

The modified device model SM' does not always have the same shape as the initial device model SM and can be fabricated more easily than the initial one. The details of the steps are explained in the sub-sections.

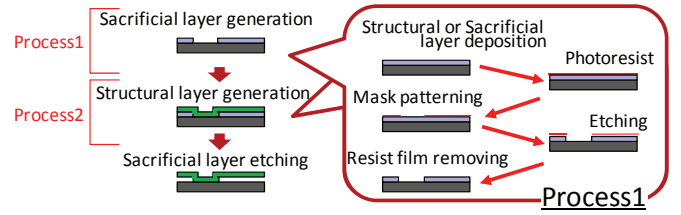


Fig.1 An overview of surface micromachining

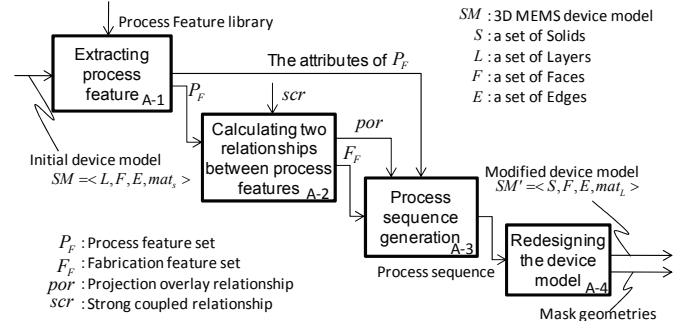


Fig.2 A flow of the process planning

2.3 Searching process features (A-1)

An initial MEMS device model SM with 3D assembly structure is given in Eq.(1).

$$SM = \langle S, F, E, mat_s \rangle \quad (1)$$

where S is a set of solids which corresponds to one connected volume of structural layers made of a single material, F a face set of faces in the device model, and E a set of edges in the device model, and $mat_s : S \rightarrow M_n$ is a material attribute of each solid S , and a set of material names M_n .

Process features are extracted based on the following steps. First, we search for a *geometric feature set* G_F in the device model. A *geometric feature* $gf \in G_F$ is defined in Eq.(2).

$$gf = \left\{ (f^t, f^m, f^b, e^{bm}, e^{bm}) \mid \begin{array}{l} f^t, f^m, f^b \in F'(s_k), \quad e^{bm}, e^{bm} \in E'(s_k), \\ s_k \in S, \quad e^{bm} = f^t \hat{\cap} f^m, \quad e^{bm} = f^b \hat{\cap} f^m \end{array} \right\} \quad (2)$$

where $F'(s_k)$ is a set of faces which belongs to a solid s_k , $E'(s_k)$ a set of edges which belong to s_k , and $e^{bm} = f^t \hat{\cap} f^m$ means that f^t and f^m share an edge e^{bm} . f^t, f^m, f^b are called “top face”, “middle face” and “bottom face”, respectively.

As shown in Fig.3, a geometric feature is either a *bend feature* or a *sidepocket feature*. They are identified according to the normal vector direction of $F'(s_k)$ and convexity/concavity of $E'(s_k)$.

Next, the following three attributes for each geometric feature are defined:

- **Material attribute** $mat : G_f \rightarrow M_n$

A material attribute value $mat(gf)$ of a geometric feature gf which belongs to a solid s_k is made identical to the material attribute value $mat_s(s_k)$.

- **Deposition thickness attribute** $t_p : G_f \rightarrow R^+$

As shown in Fig.3, a deposition thickness attribute value $t_p(gf)$ represents the minimum distance from the *topface* of the geometric feature to a horizontal face which exists above the *topface*.

- **Sacrificial layer attribute** $sac : G_f \rightarrow \{true, false\}$

A sacrificial layer attribute value $sac(gf)$ indicates, as shown in Fig.4, whether an open space exists below the *topface* of the geometric feature or not. So, $sac(gf)$ is defined as Eq.(3).

$$sac(gf) = \begin{cases} \text{true} & (\{topface(gf)\} \hat{\cap} (F - \{topface(gf)\})) \neq \emptyset \\ \text{false} & (\text{otherwise}) \end{cases} \quad (3)$$

where $topface(gf)$ means a *topface* of the gf , and $\{f_i\} \hat{\cap} \{f_j\}$ means the Boolean subtraction of two-face sets $\{f_i\}$ and $\{f_j\}$.

As shown in Fig.4, $sac(gf) = true$ means that a sacrificial layer is needed to fabricate a solid in which this geometric feature exists. In this case, the minimum value of the z-direction width of the *midleface* shown in Fig.3 is evaluated as $t_s(gf)$.

These attributes of the geometric feature gf are inherited by a *process feature* pf , and a *fabrication feature* ff generated in A-2.

In addition, the *bottom feature set* B_F is generated. A face which has a normal vector of negative-z-direction and does not belong to any geometric features is defined as a *bottom feature* $bf \in B_F$ as shown in Fig.3

Finally, by combining the geometric features and the bottom features, A *process feature set* P_F is generated as Eq.(4).

$$P_F = G_F \cup B_F \quad (4)$$

2.4 Calculating two relationships between Process Features (A-2)

In A-2, two geometric relationships among process features are calculated:

Calculating *projection overlay relationships* (*por*) among process features are tested, and its result is expressed as a *projection overlay relationship matrix* $\mathbf{A}_{P_F} = \{a_{ij}\}$. The entry a_{ij} is calculated by Eq.(5).

$$a_{ij} = \begin{cases} 1 & (topface_z(pf_i) \leq topface_z(pf_j), por(pf_i, pf_j) = true) \\ 0 & (otherwise) \end{cases} \quad (5)$$

where $topface_z(pf)$ is a z-coordinate value of the *topface*. As for a_{ij} , the process features pf_1, pf_2, pf_3, \dots are arranged in ascending order of the $topface_z(pf_i)$. This leads to entries a_{ij} for $(i > j)$ of \mathbf{A}_{P_F} being zero. As shown in Fig.5, $por(pf_i, pf_j) = true$ shows that the projections in the z-direction of two *topfaces* in pf_i and pf_j overlap each other. An example of projection overlay relationship and projection overlay relationship matrix is shown in Fig.5. $a_{ij} = 1$ in the projection overlay relationship matrix \mathbf{A}_{P_F} means that the process feature pf_i must be deposited before the process feature pf_j is done.

A *strongly coupled relationship* (*scr*) is calculated. The relationship means that an identical face is shared among more than two process features, and is evaluated by Eq.(6).

$$scr(pf_i, pf_j) = \begin{cases} true & (F'(pf_i) \cap F'(pf_j) \neq \emptyset) \\ false & (otherwise) \end{cases} \quad (6)$$

where $F'(pf_i)$ is a set of faces which belong to a process feature pf_i .

As shown in Fig.6, because the process features pf_i and pf_j are generated by the same deposition process, if $scr(pf_i, pf_j) = true$, these process features are combined into one *fabrication feature* $ff_k = \{pf_i, pf_j\}$ in the *fabrication feature set* F_F . Furthermore, the process features belonging to the same fabrication feature are also considered to have implicitly strong coupled relationships.

2.5 Process sequence generation (A-3)

2.5.1 Precedence relationship digraph generation

The *projection overlay relationship matrix* $\mathbf{A}_{F_F} = \{c_{lm}\}$ among fabrication features is calculated based on a projection overlay relationship matrix \mathbf{A}_{P_F} among process features. Entry c_{lm} is calculated by Eq.(7) based on the projection overlay relationship matrix entry a_{ij} .

$$c_{lm} = \bigvee_{pf_i \in ff_l, pf_j \in ff_m} a_{ij} \quad (7)$$

where \vee is logical sum.

After that, a *precedence relationship matrix* $\mathbf{B}_{F_F} = \{b_{lm}\}$ is calculated where the “*redundant*” relationships in projection overlay relationship have been removed. In order to do this, c_{lm} substituting into b_{lm} for all b_{lm} and c_{lm} must be completed first, and then the entries b_{lm} corresponding to the “*redundant*” relationships are set to zero.

Following this, a *precedence relationship digraph* G_A is defined which expresses the projection overlay relationship between fabrication features. A *precedence relationship digraph* G_B is also defined which expresses the precedence relationship of the deposition order between fabrication features as follows.

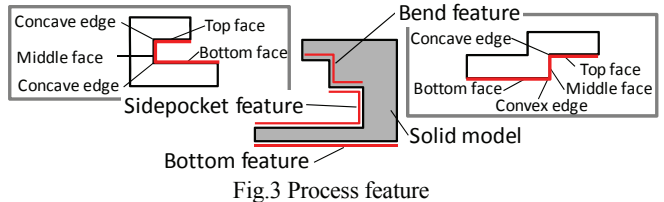


Fig.3 Process feature

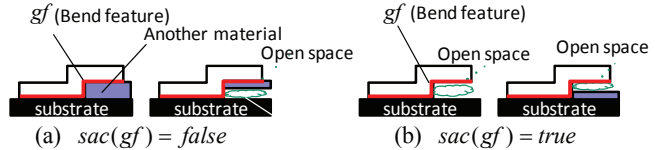


Fig.4 The relationship between process feature and sacrificial layer

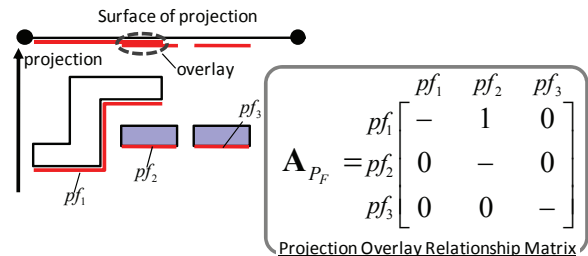


Fig.5 Projection overlay relationship and its matrix

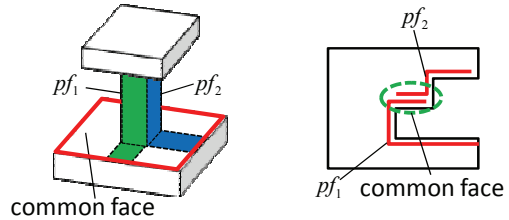


Fig.6 Strong coupled relationship

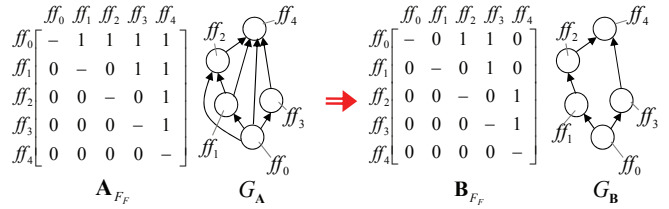


Fig.7 Precedence relationship digraph generation

$$G_A = \langle V_A, E_A \rangle, \quad \begin{cases} V_A = F_F \\ E_A = \{(ff_i, ff_j) \mid c_{ij} = 1\} \end{cases} \quad (8)$$

$$G_B = \langle V_B, E_B \rangle, \quad \begin{cases} V_B = F_F \\ E_B = \{(ff_i, ff_j) \mid b_{ij} = 1\} \end{cases}$$

where, V_A and V_B are sets of graph nodes.

An example of $\mathbf{A}_{F_F}, G_A, \mathbf{B}_{F_F}, G_B$ is shown in Fig.7. All of the redundant edges in G_A are deleted in G_B .

2.5.2 Process tree generation

For process sequence generation, a new attribute to node ff and new sets of nodes ff are generated as follows:

- **Deposited attribute** $depended : F_F \rightarrow \{true, false\}$

This attribute expresses whether each node of G_B has been deposited or not.

- **Parent nodes set** $P_G(ff_j)$

A set of ff_i the corresponding entry of which shows the precedence relationship matrix $b_{ij} = 1$ for fabrication features ff_j .

- **Deposited nodes set** $D_{ed}(G_B)$

In G_B , a set of ff_i the deposited attribute of the value $depended(ff_i)$ is *true*.

● **Depositable nodes set** $D_{cand}(G_B)$

In G_B , a set of ff_i the deposited attribute of the value $deped(ff_i) = \text{false}$ and $P_G(ff_i) \in D_{ed}(G_B)$.

After defining the attribute and the sets, a new node ff_i^s is inserted between the node ff_i and the parent nodes $P_G(ff_i)$ in G_B . In this case, for the ff_i are only used the sacrificial layer attribute of the value $Sac(ff_i) = \text{true}$. The inserted nodes are called *sacrificial node* ff_i^s , and other nodes in G_B are called *structural node* ff_i^p .

Process sequence can be generated by changing the deposited attribute value $deped(ff_i)$ of each fabrication feature ff_i in G_B . The transition of the deposited attribute state in G_B is expressed by the tree structure model. The tree structure model is called the *process tree*.

2.5.3 Exhaustive search for process sequence

In order to express whether each node in G_B has already been deposited at a certain point in the process sequence, a new digraph called *state diagram* T_i is introduced. Each node of the diagram has a deposited attribute value $deped(ff_i)$, and a difference in the attribute values of the diagram represents a different deposition state of the fabrication features which correspond to a node in the process tree.

When building the process tree, an initial state T_0 expressing a root of the tree is generated first. In T_0 , the deposited attribute value $deped(ff_0^p)$ of a fabrication feature ff_0^p belonging to substrate is set to be *true*, while those of the other features $deped(ff)$ are *false*. The deposited node set $D_{ed}(T_0)$ only includes ff_0^p . In a general state T_k , one combination of the fabrication features included in the depositable node set $D_{cand}(T_m)$ can only be built where T_m is an immediate previous state of T_k . When a certain combination of depositable features $\{ff_i\}$ satisfying the condition has been selected, a state diagram T_m changes to the next state T_k , the attribute values of $deped(ff_i)$ in $\{ff_i\}$ changes to *true* and the features $\{ff_i\}$ are added to the current depositable node set $D_{cand}(T_k)$. A new node is added to the process tree as a result of the state change. If a different combination of fabrication features can be built in T_k , then all possible alternatives of the combinations can be selected in turn, and this introduces a branch in the process tree. By repeating this exhaustive search in depth first order until the deposited attribute values of all fabrication features are *true*, a complete process tree can be generated in the system.

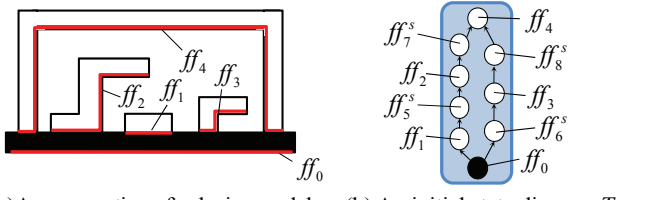
An example of the exhaustive search for a process tree is shown in Fig.8. Fig.8(a) shows a cross section of a device model composed of single material structural layers. Fig.8(b) shows the initial state diagram T_0 . In state T_0 , $D_{cand}(T_0)$ consists of ff_1^p and ff_6^s . Then, as shown in Fig.8(c), all possible next states T_1 and T_2 were derived by searching all combinations of the features ff_i included in $D_{cand}(T_0)$, the material attribute values $mat(ff_i)$ of which identical. The expansion of the process tree is shown in Fig.8(d). A leaf of the tree is a state in which attribute values $deped(ff)$ of all nodes are *true*. Each unique route of the process tree corresponds to a difference process sequence.

2.6 Redesigning the device model (A-4)

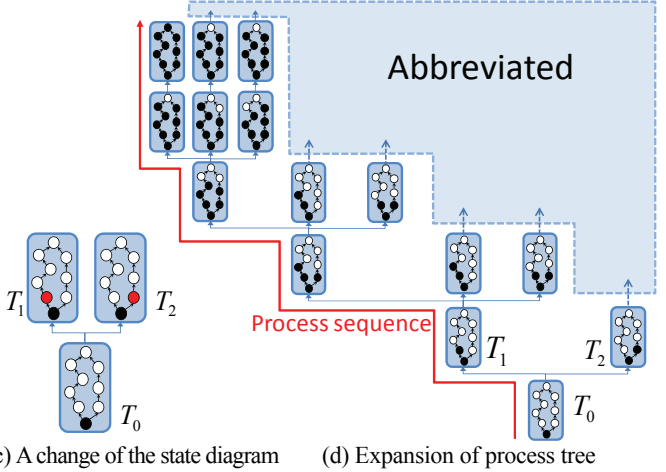
A modified device model SM' is generated in this step according to the process sequences searched for in A-3. At the beginning of the generation, the solid of the substrate in SM is copied to the one in SM' . Here, a deposition layer and a mask geometry corresponding to each process in the process sequence are estimated.

The steps for redesigning the device model at a state transition $T_i \rightarrow T_j$ is shown as the following i) ~ iv). In the steps, it is assumed that etching goes straight into the negative z-direction and removes layer portions made of a particular material that are uncovered with the resist film.

- i) A *depositing fabrication feature set* $D_{ing}(T_i, T_j)$ is defined. This is a set of the fabrication features ff the deposited attribute value changes to be *true* at this state transition $T_i \rightarrow T_j$.
- ii) Estimation of actual deposition layer shapes.
- ii-a) If a structural node is deposited in the transition, the deposition layer with minimum thickness $t_p(ff)$ is built on the already deposited layers in SM' .



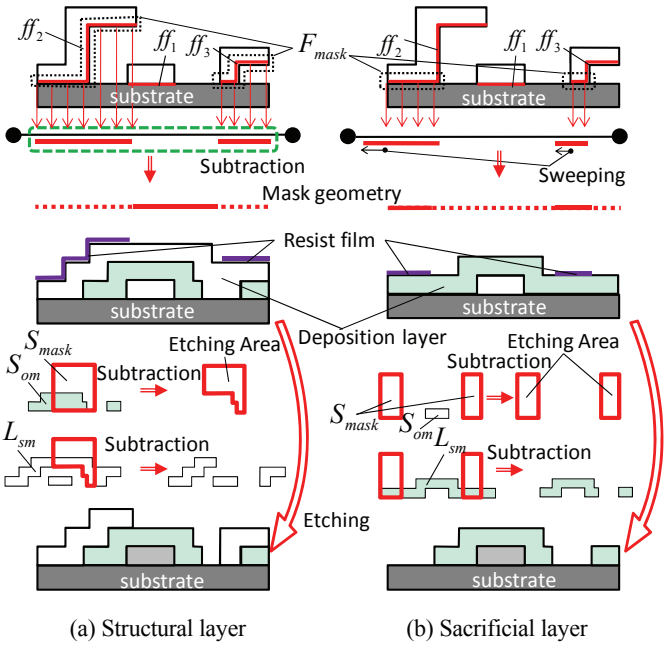
(a) A cross section of a device model (b) An initial state diagram T_0



(c) A change of the state diagram (d) Expansion of process tree

Fig.8 A state diagram and a process tree

Node color: black(deposited), red(depositing), white(undeposited)



(a) Structural layer

(b) Sacrificial layer

Fig.9 Mask face and deposited layer estimation

- ii-b) If a sacrificial node is deposited in the transition, the deposition layer with minimum thickness $t_s(ff)$ is built on the already deposited layers in SM' .
- iii) Estimation of mask faces
- iii-a) If a structural node is deposited, a *mask face set* $F_{mask} = D_{ing}(T_i, T_j)$ is generated. As shown in Fig.9(a), a 2D mask geometry is generated by Boolean subtraction of the geometry projected to the F_{mask} from a substrate surface.
- iii-b) If a sacrificial node is deposited, a mask face set $F_{mask} \in D_{ing}(T_i, T_j)$ is generated where the faces in F_{mask} are limited to be *bottomfaces* in the process features in the sacrificial layer. Then, as shown in Fig.9(b), the edges which are boundaries of the *bottomfaces* in F_{mask} and are not shared by a *middleface*, are swept in minimum thickness $t_s(ff)$ toward the direction vertical edge and parallel to the face. An mask geometry is obtained as a z-direction projected geometry of F_{mask}

iv) The shape of the modified device model SM' is estimated by applying a sequence of geometric operations simulating etching of a process to SM' as Eq.(9).

$$SM' = (L_{sm} \Delta (S_{mask} \Delta S_{om})) \hat{\cup} L_{om} \quad (9)$$

where L_{sm} is a set of the deposition layers and deposited layers the material attribute values of which are identical to the deposition layer's ones, L_{om} a set of the deposited layers the material attribute values of which are not identical to the deposition layer's ones, S_{mask} a volume made by sweeping the mask geometry toward the z-direction, S_{om} a swept volume of L_{om} to z-direction, Δ Boolean difference and $\hat{\cup}$ Boolean sum.

By repeating the above steps i)-iv) and finally removing the sacrificial layers, the modified device model SM' , which is easier to fabricate than the initial one can be automatically obtained.

3. A case study

The proposed process planning system was implemented using Parasolid[8] which is a commercial 3D solid modeling toolkit. Its solid modeling functions enabled effective implementation of the planning system.

The effectiveness of the process planning system was verified by a case study for the device model of a micro-oxide-sensor[9]. The sensor is composed of layers made of Si_3N_4 , Pt and ZrO_2 . Electrode and a heater are made of Pt, a chamber structure with a small orifice is made of Si_3N_4 , and ZrO_2 an ionic conductor of O^- as shown in the initial device model Fig.10(a). The device model consists of five solids corresponding to the device layers.

Our planning system detected 27 process features and derived three different process sequences. Fig.10(b) shows a change of the 3D geometries of the device in one process sequence with minimum fabrication processes, and Fig.10(c) is the modified device model for the initial model. The time required for this exhaustive search of the sequence took only 6 seconds in the system using a standard PC.

By comparing Fig.10(a) to Fig.10(c), it was shown that the modified model Fig.10(c) had a small differences in shape near the electrode and heater but kept all functions of the sensor included in the initial device model unchanged. This could be fabricated more easily than Fig.10(a).

To verify the correctness of the derived process sequence from our planning system, MemsONE[4] was used. The process sequence and a set of the mask geometries derived from the planning system were inputted into the simulator, and MemsONE, and the change of the estimated 3D geometries of the device model during the step by step processes was outputted in MemsONE. By comparing the change of geometries of the model from the simulator and that from our planning system, it was verified that our derived process sequence could realize the 3D geometries of the modified device model.

From these results, basic functionality, effectiveness and efficiency of the proposed process planning algorithm for MEMS devices have been verified.

4. Conclusions and future works

A prototype of a new 3D process planning system for MEMS device manufacturing was developed in the paper. The search algorithm for all possible process sequences using the feature recognition technique in a 3D device model was proposed. A redesign algorithm of modifying some portions of the device model into easier ones to be fabricated was also proposed. A case study of process planning for a micro oxide sensor indicated that the derived process plan and redesigned model based on the algorithms were plausible and that the planning could be finished in a short time.

However, a small number of irrelevant process sequences were still derived from the system which did not fit constrains on depositions and etchings. Therefore, in our future works, the function that can precisely eliminate these irrelevant sequences will be added to the system. And furthermore, the function that can treat fabrication processes other than surface micromachining will also be realized.

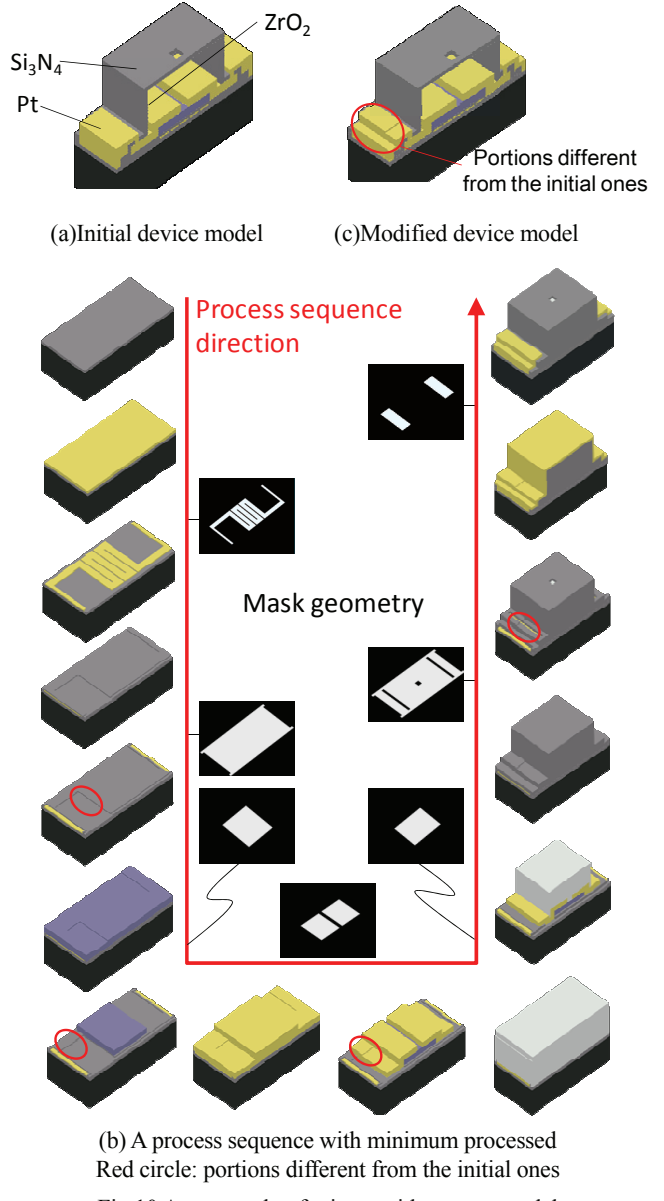


Fig.10 A case study of micro-oxide-sensor model

REFERENCES

1. Jiang, T. and Blanton, R., "Inductive Fault Analysis of Surface-Micromachined MEMS", IEEE Transactions on Computer-Aided Design of Integrated Circuits and Systems, Vol. 25, No. 6, pp. 1104-1116, 2006.
2. Zhou, Z., Huang, Q., Li, W. and Lu, W. "A Novel 3-D Dynamic Cellular Automata Model for Photoresist-Etching Process Simulation", IEEE Transactions on Computer-Aided Design of Integrated Circuits and Systems, Vol. 26, No. 1, pp. 100-113, 2007.
3. CoventorWare, Available, <http://www.coventor.com/index.html>
4. MemesONEver.1.2, Available, <http://mmc.la.coocan.jp/mems-one>
5. Li, J., Gao, S. and Liu, Y., "Solid-based CAPP for surface micro-machined MEMS devices," Computer-Aided Design, Vol. 39, No. 2, pp.190-201, 2007.
6. Jawalkar, S. and Campbell, M., "Automated synthesis of MEMS fabrication sequences using graph grammars," Proc. ASME IDETC/CIE, DETC2007-34691, 2007.
7. Cho, S., Lee, K. and Kim, T., "Development of a geometry-based process planning system for surface micromachining," International Journal of Production Research, Vol. 40, No. 5, pp. 1275-1293, 2002.
8. Parasolid, Available, http://www.plm.automation.siemens.com/en_us/products/open/parasolid/index.shtml
9. Gad-el-Hak, M., "MEMS Design and Fabrication," CRC Press, chapter11, p15, 2006.